Journal of Sound and Vibration (1997) **200**(5), 563–577

DYNAMIC RESPONSE OF NON-UNIFORM COMPOSITE BEAMS

S. Ramalingeswara Rao and N. Ganesan

Machine Dynamics Laboratory, Department of Applied Mechanics, Indian Institute of Technology, Madras 600 036, *India*

(*Received* 10 *November* 1994, *and in final form* 11 *December* 1995)

The harmonic response of tapered composite beams is investigated by using a finite element model. Only uniaxial bending is considered. The Poisson effect is incorporated in the formulation of the beam constitutive equations. Interlaminar stresses are evaluated by using stress equilibrium equations. The effects of in-plane inertia and rotary inertia are also considered in the formulation of the mass matrix. A parametric study is carried out to investigate the influence of taper profile and taper parameter. Linearly varying thickness variations of increasing, decreasing, decreasing–increasing and increasing–decreasing types are considered.

1. INTRODUCTION

Conventional metals are being replaced by fibre-reinforced composite materials in a variety of structural components owing to their high strength-to-weight and stiffness-to-weight ratios. Non-uniform beams, tapered and stepped, can be used to achieve a better distribution of strength and weight and sometimes to satisfy architectural and functional requirements. Nowadays the interest in laminated beams, uniform and non-uniform, is growing, as they are finding a number of applications such as turbine blades, helicopter blades, robot arms, etc. The analysis of composite structures is a complex task due to the bending–extension coupling. These structures are very often subjected to a dynamic environment, necessitating better understanding of the vibration characteristics. The dynamic analysis of laminated beams is mostly restricted to eigenvalue analysis.

A review of the literature (see, e.g., reference [1]) indicates that little work has been carried out on the finite element analysis of composite beams, compared to plates. Yuan and Miller [2, 3] have developed beam finite elements. The models include separate rotational degrees of freedom for each lamina, but do not require additional axial or transverse degrees of freedom beyond those necessary for a single lamina. A set of higher order theories, with C^0 finite elements having five, six and seven degrees of freedom per node, for the analysis of composite and sandwich beams has been presented by Manjunatha and Kant [4]. An interlaminar stress continuity theory via the multi-layer approach has been presented by Lee and Liu [5]. This theory satisfies the continuity equations of both interlaminar shear stresses and interlaminar normal stresses at a composite interface. The effect of non-uniformity has been discussed by several authors. The paper by Karabalis and Beskos [6] contains a comprehensive list of references on the subject. Oral [7] has formulated a three-noded finite element, with six degrees of freedom per node, three displacements and three independent rotations, for a linearly tapered symmetrically laminated composite beam using first order shear deformation theory. This

0022–460X/97/100563 + 15 $25.00/0/sv950620

element is obtained from a five-node parent element [2] by constraining the shear angle variation along the length to be linear.

The paper by Kapania and Raciti [1] describes recent developments in the vibration analysis of laminated composite beams. In recent years, several authors have tried to predict the natural frequencies of laminated beams of uniform thickness. Miller and Adams [8] studied the vibration characteristics of orthotropic clamped–free beams using classical lamination theory. Vinson and Sierakowiski [9] have given exact solutions based on classical lamination theory. Chen and Yang [10] and Chandrashekhara *et al*. [11] have carried out the free vibration analysis of composite beams based on first order shear deformation theory. Recently, Chandrashekhara and Bangera [12] have studied the free vibration characteristics of laminated composite beams using a third order shear deformation theory. They have corrected generalized force and generalized strain relations, to consider the Poisson effect, by ignoring the forces in the y direction. This operation involves inversion of certain matrices and is limited to the type of beam theory that one is using. It would be appropriate to correct stress–strain relations rather than to correct the generalized force and generalized strain relations [13].

In the present work, the dynamical behaviour of tapered composite beams subjected to a point harmonic excitation is studied by using a finite element method. Results are obtained with both first order and third order shear deformation theories. The Poisson effect is incorporated by correcting stress–strain relations. The effects of in-plane inertia and rotary inertia are also considered in the formulation of the mass matrix. Only uniaxial bending is considered. Interlaminar stresses are evaluated using equilibrium equations. A variety of parametric studies are conducted to demonstrate the influence of the taper on the response.

2. FORMULATION

The following displacement equations [14] are used in obtaining one-dimensional laminated beam equations:

$$U(x, z, t) = u(x, t) + z[\psi_x(x, t) - (4/3)(z/h)^2(\psi_x(x, t) + \partial w(x, t)/\partial x)],$$
$$W(x, z, t) = w(x, t). \tag{1}$$

Here u and w are in-plane and lateral displacements of the middle surface, ψ_x is the rotation of the normal to the middle plane about the y-axis, and h is the thickness of the beam.

The strains associated with the displacements in equation (1) are

$$\varepsilon_x = \varepsilon_x^0 + z[k_x^1 + z^2 k_x^2], \qquad \gamma_{xz} = \gamma_{xz}^* + z^2 k_{xz}^*, \tag{2}$$

where

$$\varepsilon_x^0 = \partial u/\partial x, \qquad \gamma_{xz}^* = \psi_x + \partial w/\partial x, \qquad k_x^1 = \partial\psi_x/\partial x,$$
$$k_{xz}^* = -(4/h^2)(\psi_x + \partial w/\partial x), \qquad k_x^2 = -(4/3h^2)(\partial\psi_x/\partial x + \partial^2 w/\partial x^2).$$

The stresses in the nth layer, the principal material axis of which is oriented at an angle θ to the x-axis, are related to the strains by the relation

$$\begin{Bmatrix} \sigma_{xx} \\ \sigma_{yy} \\ \sigma_{zz} \\ \tau_{yz} \\ \tau_{xz} \\ \tau_{xy} \end{Bmatrix} = \begin{bmatrix} C_{11} & C_{12} & C_{13} & 0 & 0 & C_{16} \\ C_{12} & C_{22} & C_{23} & 0 & 0 & C_{26} \\ C_{13} & C_{23} & C_{33} & 0 & 0 & C_{36} \\ 0 & 0 & 0 & C_{44} & C_{45} & 0 \\ 0 & 0 & 0 & C_{45} & C_{55} & 0 \\ C_{16} & C_{26} & C_{36} & 0 & 0 & C_{66} \end{bmatrix} \begin{Bmatrix} \varepsilon_{xx} \\ \varepsilon_{yy} \\ \varepsilon_{zz} \\ \gamma_{yz} \\ \gamma_{xz} \\ \gamma_{xy} \end{Bmatrix}. \tag{3}$$

If the beam is undergoing uniaxial bending and if there is no torsional loading, one can take $\sigma_{yy} = \sigma_{zz} = \tau_{yz} = \tau_{xy} = 0$. Upon substituting in equation (3) one arrives at the following relation which would account for Poisson effect [10]:

$$\begin{Bmatrix} \sigma_{xx} \\ \tau_{xz} \end{Bmatrix} = \begin{bmatrix} Q_{11} & 0 \\ 0 & Q_{55} \end{bmatrix} \begin{Bmatrix} \varepsilon_{xx} \\ \gamma_{xz} \end{Bmatrix}. \tag{4}$$

Here $Q_{11} = C^*_{11} - C^*_{16}C^*_{16}/C^*_{66}$ and $Q_{55} = C^*_{55}$. The relations for C^*_{ij} in terms of C_{ij} are given in reference [10].

2.1. STRAIN ENERGY

The stiffness matrix is formulated by using the strain energy expression for the beam, given by

$$U = \tfrac{1}{2}\int_{\mathrm{vol}} (\sigma_{xx}\varepsilon_{xx} + \tau_{xz}\gamma_{xz})\,\mathrm{d\,vol}, \qquad U = \tfrac{1}{2}\int_0^1 \{\varepsilon_0\}^{\mathrm{T}}\{N_0\}\,\mathrm{d}x, \tag{5}$$

where

$$\{\varepsilon_0\}^{\mathrm{T}} = [\varepsilon_x^0 \quad k_x^1 \quad k_x^2 \quad \gamma^*_{xz} \quad k^*_{xz}], \qquad \{N_0\}^{\mathrm{T}} = [N_x \quad M_x \quad P_x \quad Q_{xz} \quad R_{xz}].$$

Upon expressing the generalized stress vector as $\{N_0\} = [D]\{\varepsilon_0\}$ and substituting in equation (5), the expression for the strain energy becomes

$$U = \tfrac{1}{2}\int_0^1 \{\varepsilon_0\}^{\mathrm{T}}[D]\{\varepsilon_0\}\,\mathrm{d}x, \tag{6}$$

where

$$[D] = \begin{bmatrix} A_{11} & B_{11} & E_{11} & 0 & 0 \\ B_{11} & D_{11} & F_{11} & 0 & 0 \\ E_{11} & F_{11} & H_{11} & 0 & 0 \\ 0 & 0 & 0 & A_{55} & D_{55} \\ 0 & 0 & 0 & D_{55} & F_{55} \end{bmatrix},$$

$$(A_{ij}, B_{ij}, D_{ij}, E_{ij}, F_{ij}, H_{ij}) = b\sum_{k=1}^{nl}\int_{h_{k-1}}^{h_k} Q_{ij}(1, z, z^2, z^3, z^4, z^5)\,\mathrm{d}z.$$

Taper is considered for the thickness with the width of the beam kept constant. Only symmetrically tapered beams of rectangular cross-section are considered. Different tapered beams are obtained from a uniform beam by altering the thickness of each layer along the length and keeping its length, width and volume constant. For a tapered beam defined by a function $f(x)$ and for any particular taper parameter β, the thickness h_k of the kth layer at any distance x can be calculated by using the relation

$$h_k = (h_1)_k\{1 - \beta f(x)\}, \tag{7}$$

where β is the taper parameter, $=(1 - h_2/h_1)$, h_1 is the maximum half-thickness of the tapered beam, h_2 is the minimum half-thickness of the tapered beam and $f(x)$ is a function defining the taper profile. In equation (7) the only unknowns are $(h_1)_k$, which can be calculated by equating the volume enclosed between the kth interface (or face) and the middle surface of the tapered beam to the corresponding volume of the uniform beam.

TABLE 1

Comparison of natural frequencies (kHz) *of a simply supported orthotropic* (0°) *graphite–epoxy beam*

L/h	Mode no.	CLT [9]	FSDT [11]	Present FSDT	HSDT [12]	Present HSDT
120 ($L = 762$ mm)	1	0·051	0·051	0·051	0·051	0·051
	2	0·203	0·203	0·202	0·202	0·202
	3	0·457	0·454	0·452	0·453	0·454
	4	0·812	0·804	0·798	0·799	0·804
	5	1·269	1·262	1·236	1·238	1·252
15 ($L = 381$ mm)	1	0·813	0·755	0·753	0·756	0·754
	2	3·250	2·548	2·545	2·554	2·555
	3	7·314	4·716	4·714	4·742	4·753
	4	13·002	6·960	7·021	7·032	7·052
	5	20·316	9·194	9·201	9·355	9·382

2.2. KINEMATIC ENERGY

The expression for the kinematic energy may be written as

$$T = \tfrac{1}{2} \int_{\mathrm{vol}} \rho(\dot{U}^2 + \dot{W}^2)\, \mathrm{d\,vol}. \tag{8}$$

2.3. ELEMENT MATRICES

For the finite element formulation a two-node beam element with four degrees of freedom $[u_j \; w_j \; (\partial w/\partial x)_j \; \psi_{xj}]$ per node is used. For this configuration the generalized displacements are interpolated by using expressions of the form

$$u(x, t) = \sum_{j=1}^{2} u_j(t) N_j(x), \qquad \psi_x(x, t) = \sum_{j=1}^{2} \psi_{xj}(t) N_j(x),$$

$$w(x, t) = \sum_{j=1}^{2} \{w_j(t)\zeta_j(x) + (\partial w(t)/\partial x)_j \xi_j(x)\}, \tag{9}$$

where N_j are the Lagrange linear interpolation functions, whereas $\zeta_j(x)$ and $\xi_j(x)$ are Hermite cubic interpolation functions. By using equation (9) the generalized strains can be expressed as

$$\{\epsilon_0\} = [B]\{\delta_e\}, \tag{10}$$

TABLE 2

Tip displacements of the tapered isotropic beam (in)

	Bending			Stretching		
D/d	Reference [8]	Present HSDT	Present FSDT	Reference [7]	Present HSDT	Present FSDT
2	0·02729	0·02782	0·02780	0·23077E − 03	0·2310E − 03	0·2310E − 03
5	0·04789	0·04856	0·04854	0·32609E − 03	0·3350E − 03	0·3350E − 03

TABLE 3

Comparison of non-dimensional dynamic displacements of a simply supported isotropic beam of uniform thickness

	$x = L/4$			$x = L/2$		
Mode no.	Reference [15]	Present HSDT	Present FSDT	Reference [15]	Present HSDT	Present FSDT
1	100	97·47	99·98	141·40	137·84	141·38
2	12·50	12·58	12·49	—	0·1191	0·1524
3	1·2350	1·2608	1·2325	1·746	1·7821	1·7421

where $[B]$ is the matrix of shape functions and their derivatives and $\{\delta_e\}$ is the nodal displacement vector. The element stiffness matrix $[K]_e$ can be obtained by substituting equation (10) in equation (6), whereas the element mass matrix $[M]_e$ can be obtained by substituting equation (9) in equation (8):

$$[K]_e = \int_0^1 [B]^{\mathrm{T}}[D][B]\,\mathrm{d}x, \qquad [M]_e = \int_0^1 [N]^{\mathrm{T}}[\rho][N]\,\mathrm{d}x.$$

Here $[N]$ is the matrix of shape functions and its derivatives.

2.4. STEADY STATE RESPONSE

The natural frequencies are obtained by solving the eigenvalue problem

$$[K]\{\delta\} = \omega^2[M]\{\delta\}, \tag{11}$$

where $[K]$ and $[M]$ are the global stiffness and the global mass matrices respectively, δ is the corresponding eigenvector and ω is the natural frequency.

For a small amount of structural damping, the steady state response of a beam subjected to harmonic excitation is given by

$$[K_d]\{U\} = \{F\}, \tag{12}$$

where $[K_d]$ is the dynamic stiffness matrix given by

$$[K_d] = [K](1 + \eta\mathrm{i}) - \Omega^2[M],$$

TABLE 4

Normalized results for a simply supported [0/90/0] *beam under sinusoidal loading*

	$L/h = 4$			$L/h = 20$			$L/h = 40$		
	w	τ_{xz}	σ_z	w	τ_{xz}	σ_z	w	τ_{xz}	σ_z
Present HSDT	2·700	1·610	0·5086	0·6024	8·882	0·4944	0·5336	17·82	0·4939
Present FSDT	2·411	1·800	0·500	0·5867	9·002	0·5000	0·5296	18·00	0·5000
Reference [5]	2·887	1·431	0·4988	0·6172	8·749	0·5001	0·5367	17·63	0·5000

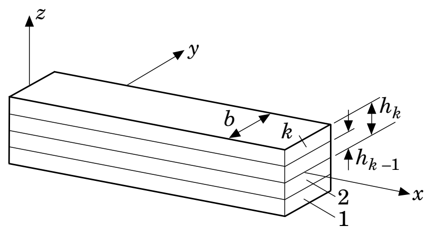

Figure 1. A straight uniform composite beam.

in which $\{F\}$ is the force vector consisting of the amplitudes of the nodal forces, $\{U\}$ is the displacement vector, Ω is the frequency of excitation and η is the structural damping factor.

The dynamic displacements $\{U\}$ obtained from equation (12) are then used to obtain dynamic in-plane stresses by using equations (2), (4) and (9).

2.5. EVALUATION OF DYNAMIC TRANSVERSE STRESSES

It is to be noted that in the case of ESL theories the transverse stresses evaluated by using constitutive equations are not correct. The transverse stresses can be determined with reasonable accuracy from the following stress equilibrium equations in the absence of body forces:

$$\partial\sigma_{xx}/\partial x + \partial\tau_{xz}/\partial z = 0, \qquad \partial\sigma_{zz}/\partial z + \partial\tau_{xz}/\partial x = 0. \tag{13}$$

To evaluate the transverse stresses through the thickness the above equilibrium equations are transformed into appropriate finite difference expressions [15]. Since the dynamic in-plane stress can be evaluated at any point across the thickness with reasonable accuracy, transverse stresses at any point across the thickness can be evaluated by using a finite

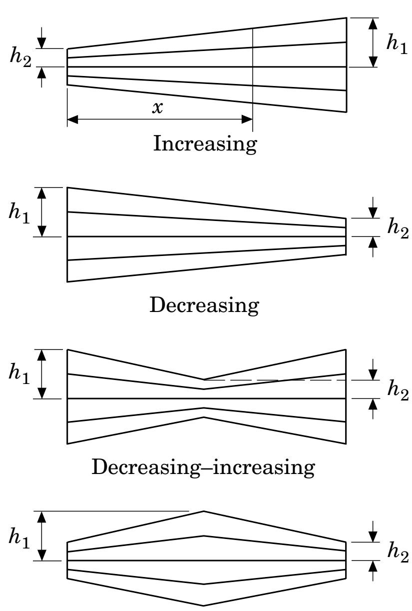

Figure 2. Different taper profiles.

TABLE 5

Non-dimensionalized frequencies (ω^*) of various taperes SS beams

Type of beam	β	Mode 1 HSDT	Mode 1 FSDT	Mode 2 HSDT	Mode 2 FSDT	Mode 3 HSDT	Mode 3 FSDT
I	0·0	2·4977	2·4961	8·4863	8·4701	15·8082	15·7478
II	0·25	2·4815	2·4798	8·4650	8·4488	15·7758	15·7142
	0·50	2·4065	2·4054	8·3671	8·3514	15·6168	15·5575
	0·75	2·1787	2·1776	8·0541	8·0418	15·1074	15·0559
III	0·25	2·4815	2·4798	8·4650	8·4488	15·7758	15·7142
	0·50	2·4065	2·4054	8·3671	8·3514	15·6168	15·5575
	0·75	2·1787	2·1776	8·0541	8·0418	15·1074	15·0559
IV	0·25	2·3606	2·3595	8·4298	8·4135	15·8015	15·7411
	0·50	2·0902	2·0897	8·1885	8·1728	15·7623	15·7052
	0·75	1·5120	1·5164	7·4591	7·4451	15·7209	15·6767
V	0·25	2·5823	2·5812	8·4410	8·4247	15·7898	15·7271
	0·50	2·6175	2·6170	8·2148	8·1986	15·6996	15·6381
	0·75	2·5050	2·5050	7·5028	7·4888	15·3778	15·3212

I, Uniform beam; II, increasing type; III, decreasing type; IV, decreasing–increasing type; V, increasing–decreasing type.

difference technique. The central difference technique is used across the thickness and the forward difference technique is used along the length.

3. RESULTS AND DISCUSSION

A number of examples have been considered. Unless mentioned otherwise, the following AS4/3051-6 graphite-epoxy material properties are used: $E_1 = 144{\cdot}80$ GPa; $E_2 = 9{\cdot}65$ GPa;

TABLE 6

Maximum displacement (w^*) values for various tapered SS beams subjected to harmonic excitation

Type of beam†	β	Mode 1 HSDT		Mode 1 FSDT		Mode 2 HSDT		Mode 2 FSDT		Mode 3 HSDT		Mode 3 FSDT	
I	0·0	49·95	21	49·93	21	6·122	11	6·116	11	1·248	21	1·252	21
II	0·25	53·47	20	53·44	20	6·860	11	6·854	11	1·298	7	1·303	7
	0·50	61·98	19	61·93	19	8·268	10	8·262	10	1·387	7	1·394	7
	0·75	88·64	17	88·53	17	11·62	9	11·61	9	1·443	6	1·459	6
III	0·25	48·23	22	48·20	22	6·155	31	6·149	31	1·342	35	1·344	35
	0·50	48·53	23	48·50	23	6·412	32	6·407	32	1·529	35	1·530	35
	0·75	55·80	25	55·75	25	7·304	33	7·296	33	1·977	36	1·974	36
IV	0·25	59·54	21	59·48	21	6·204	11	6·198	11	1·379	21	1·380	21
	0·50	83·69	21	83·50	21	6·623	12	6·618	12	1·603	21	1·598	21
	0·75	189·9	21	187·9	21	8·114	13	8·100	13	2·074	21	1·993	21
V	0·25	44·17	21	44·14	21	6·174	11	6·168	11	1·281	7	1·287	7
	0·50	40·21	21	40·19	21	6·549	10	6·544	10	1·348	7	1·357	7
	0·75	40·43	21	40·41	21	7·947	9	7·933	9	1·460	6	1·470	6

† I–V as in Table 5.

TABLE 7

Maximum stresses (σ_x^*) for various tapered SS beams subjected to harmonic excitation

Type of beam†	β	Mode 1 HSDT		Mode 1 FSDT		Mode 2 HSDT		Mode 2 FSDT		Mode 3 HSDT		Mode 3 FSDT	
I	0·0	39·65	20	38·82	20	14·87	10	13·73	10	5·130	7	4·343	7
	0·25	42·44	18	41·58	18	16·45	10	15·27	10	5·343	7	4·606	7
II	0·50	49·18	15	48·24	15	19·40	8	18·21	8	5·673	6	5·037	6
	0·75	71·58	10	70·41	10	26·82	6	25·64	6	5·860	5	5·460	5
III	0·25	38·28	23	37·51	23	14·75	31	13·70	31	5·524	34	4·756	34
	0·50	38·51	26	37·79	26	15·04	33	14·11	33	6·259	35	5·535	35
	0·75	45·05	31	44·34	31	16·86	35	16·11	35	8·047	36	7·403	36
IV	0·25	51·56	20	50·89	20	15·09	12	13·97	12	5·535	20	4·794	20
	0·50	79·45	20	79·08	20	16·13	13	15·00	13	6·243	20	5·583	20
	0·75	191·4	20	191·5	20	20·23	16	19·05	16	7·472	20	6·801	20
V	0·25	32·79	17	31·92	16	15·03	9	13·91	9	5·131	7	4·368	6
	0·50	29·51	12	28·63	12	15·99	8	14·85	8	5·255	6	4·534	6
	0·75	32·94	6	31·76	7	19·89	5	18·71	5	5·726	4	5·144	4

† I–V as in Table 5.

$G_{23} = 3{\cdot}45$ GPa; $G_{12} = G_{13} = 4{\cdot}14$ GPa; $\nu = 0{\cdot}3$; $\rho = 1389{\cdot}23$ kg/m^3. The non-dimensional parameters used in presenting results are as follows:

$$\omega = \omega L^2 \sqrt{\rho / E_1 h^2};$$

$$w^* = \frac{\text{max. dynamic displacement } w \text{ of a uniform or tapered beam}}{\text{max. static displacement } w \text{ of a uniform beam obtained with FSDT}};$$

$$\sigma_x^* = \frac{\text{max. dynamic normal stress } \sigma_x \text{ of a uniform or tapered beam}}{\text{max. static normal stress } \sigma_x \text{ of a uniform beam obtained with FSDT}};$$

$$\tau_{xz}^* = \frac{\text{max. dynamic shear stress } \tau_{xz} \text{ of a uniform or tapered beam}}{\text{max. static shear stress } \tau_{xz} \text{ of a uniform beam obtained with FSDT}};$$

$$\sigma_z^* = \frac{\text{max. dynamic normal stress } \sigma_z \text{ of a uniform or tapered beam}}{\text{max. static normal stress } \sigma_z \text{ of a uniform beam obtained with FSDT}};$$

In Table 1 the natural frequencies of a simply supported orthotropic (0°) graphite–epoxy beam are compared with existing results. The comparison is quite good. It is well known that the classical theory overpredicts the natural frequencies of thick beams. For checking the accuracy of the present formulation for tapered beams, linearly tapered clamped–free isotropic beams with decreasing thickness variation and of rectangular cross-section are analyzed for stretching and bending modes. Two beams, one with $h_1/h_2 = 2$ and the other with $h_1/h_2 = 5$, were taken for analysis. The following properties were used: $E = 30 \times 10^6$ lb/in^2; $\nu = 0$; $L = 10$ in; $b = 1$ in. The force is applied at the tip and is equal to 1000 lb. The tip displacements are compared in Table 2. The comparison is good. To validate the present formulation for the dynamic analysis the non-dimensional dynamic displacements of a simply supported isotropic beam of uniform thickness subjected to a

TABLE 8

Maximum stresses (τ_{xz}^*) *for various tapered* SS *beams subjected to harmonic excitation*

Type of beam†	β	Mode 1				Mode 2				Mode 3			
		HSDT		FSDT		HSDT		FSDT		HSDT		FSDT	
I	0·0	30·05	0	30·12	0	21·29	0	21·54	0	10·05	0	10·34	0
II	0·25	36·31	0	36·39	0	24·19	0	24·43	0	10·45	0	10·70	0
	0·50	48·89	0	48·93	0	29·32	0	29·48	0	10·90	0	11·10	0
	0·75	85·41	0	84·79	0	40·61	0	40·40	0	10·57	0	10·66	0
III	0·25	32·74	41	32·82	41	21·70	41	21·91	41	10·81	41	11·06	41
	0·50	38·27	41	38·32	41	22·72	41	22·84	41	12·03	41	12·18	41
	0·75	53·74	41	53·39	41	25·52	41	25·37	41	14·51	41	14·46	41
IV	0·25	29·28	7	29·36	7	23·82	21	24·32	21	9·970	15	10·22	15
	0·50	52·41	22	51·92	22	29·12	21	30·20	21	10·18	16	10·35	16
	0·75	205·6	22	200·3	20	43·34	21	46·22	21	10·68	19	10·33	23
V	0·25	34·61	0	34·73	0	24·13	0	24·37	0	10·71	0	10·98	0
	0·50	43·31	0	43·30	0	29·32	0	29·42	0	11·69	0	11·88	0
	0·75	64·66	0	63·12	0	41·38	41	40·44	0	13·06	0	12·90	0

† I–V as in Table 5.

point harmonic excitation at the first three natural frequencies, are compared with the analytical solutions given in reference [16]. The force is applied at one-quarter span. The comparison is shown in Table 3. The non-dimensional displacement is given by $w(x)\pi^4 EI/PL^3$, where E is Young's modulus, I is the moment of inertia, P is the magnitude of the harmonic force and L is the length of the beam. The hysteretic damping constant is taken as 0·01. The results obtained by the present formulation are in good agreement with those in reference [15]. In Table 4 the interlaminar stresses obtained with the present

TABLE 9

Maximum stresses (σ_x^*) *for various tapered* SS *beams subjected to harmonic excitation*

Type of beam†	β	Mode 1				Mode 2				Mode 3			
		HSDT		FSDT		HSDT		FSDT		HSDT		FSDT	
I	0·0	3·532	20	3·531	20	5·107	10	5·084	10	3·537	10	3·543	10
II	0·25	3·731	17	3·728	17	5·335	30	5·333	30	3·569	30	3·583	30
	0·50	4·301	10	4·282	10	5·740	28	5·740	28	3·494	28	3·522	28
	0·75	11·83	1	11·70	1	6·050	26	6·052	26	2·885	26	2·935	26
III	0·25	3·364	24	3·363	24	4·913	11	4·890	11	3·701	11	3·708	11
	0·50	3·256	31	3·252	31	4·452	13	4·452	13	3·866	13	3·878	13
	0·75	7·443	40	7·366	40	3·803	15	3·804	15	4·066	15	4·036	15
IV	0·25	21·34	20	21·37	20	5·045	11	5·026	11	4·965	11	4·972	11
	0·50	53·06	20	53·08	20	5·121	16	5·102	25	6·385	16	6·385	25
	0·75	130·2	20	128·6	20	9·362	19	9·080	19	6·678	19	6·451	19
V	0·25	11·05	20	11·07	20	5·043	10	5·023	10	3·571	10	3·588	10
	0·50	27·12	20	27·11	20	5·123	5	5·102	5	3·693	5	3·720	5
	0·75	45·38	20	45·30	20	11·81	1	11·38	1	4·577	1	4·586	1

† I–V as in Table 5.

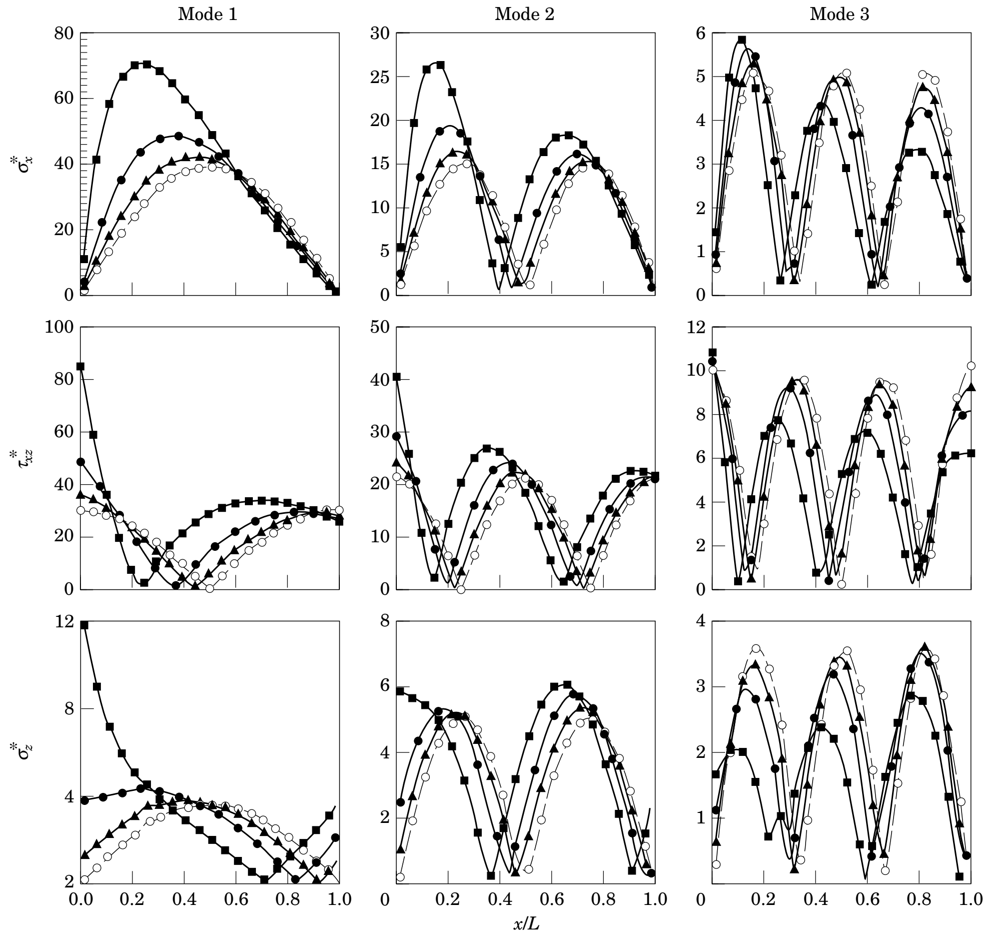

Figure 3. The variation of stresses along the length of the simply supported laminated beam of increasing thickness variation. [0/90/90/0], $L/h = 15$. h_x values: —○—○—, 0·0; —▲—▲—, 0·25; —●—●—, 0·5; —■—■—, 0·75.

formulation for the static case are compared. The comparison shows that the present results are in good agreement with the existing results.

3.1. RESPONSE OF TAPERED BEAMS

The following discussion deals with the steady state response of simply supported composite beams subjected to a point harmonic excitation at one-quarter span from the left end. The beams are excited at the first three natural frequencies and the amplitude of the load is taken to be the same in each case. For harmonic response the structural damping factor is taken as 0·02. Different taper profiles considered are shown in Figure 2, and their mathematical expressions are given in the Appendix.

The frequency values of various tapered beams are presented in Table 5. The maximum response values of various tapered beams subjected to harmonic excitation are presented in Tables 6–9. The variations of the stresses, obtained with the higher order shear deformation theory, along the length of the beam, are shown in Figures 3–6. The variation of the interlaminar stresses τ_{xz} and σ_z, along the length, shown in Figures 3–6, can be interpreted by using stress equilibrium equations. The magnitude of shear stress developed at any section depends on the slope of σ_x with respect to x at that section. As the slope of σ_x increases, the magnitude of the shear stress developed also increases, and vice versa. The shear stress is zero at that section at which the slope of σ_x is zero. σ_z is zero at that section at which the slope of τ_{xz} with respect to x is zero. The magnitude of σ_z increases as the slope of τ_{xz} increases, and vice versa.

3.1.1. *Effect of taper profile*

For any particular taper parameter and for the point harmonic load acting at one-quarter span, the transverse displacement w_{max} obtained with the increasing–decreasing thickness variation is lower than that of a uniform beam, whereas the w_{max} obtained with other thickness variations considered is higher than that of a uniform beam. Among all thickness variations considered, decreasing–increasing thickness variation results in a larger deflection. A similar trend as that observed for w_{max} is also observed for σ_x. The maximum transverse displacement and maximum normal stress σ_x developed in the decreasing beam with taper parameter less than 0·5 is slightly less than those developed

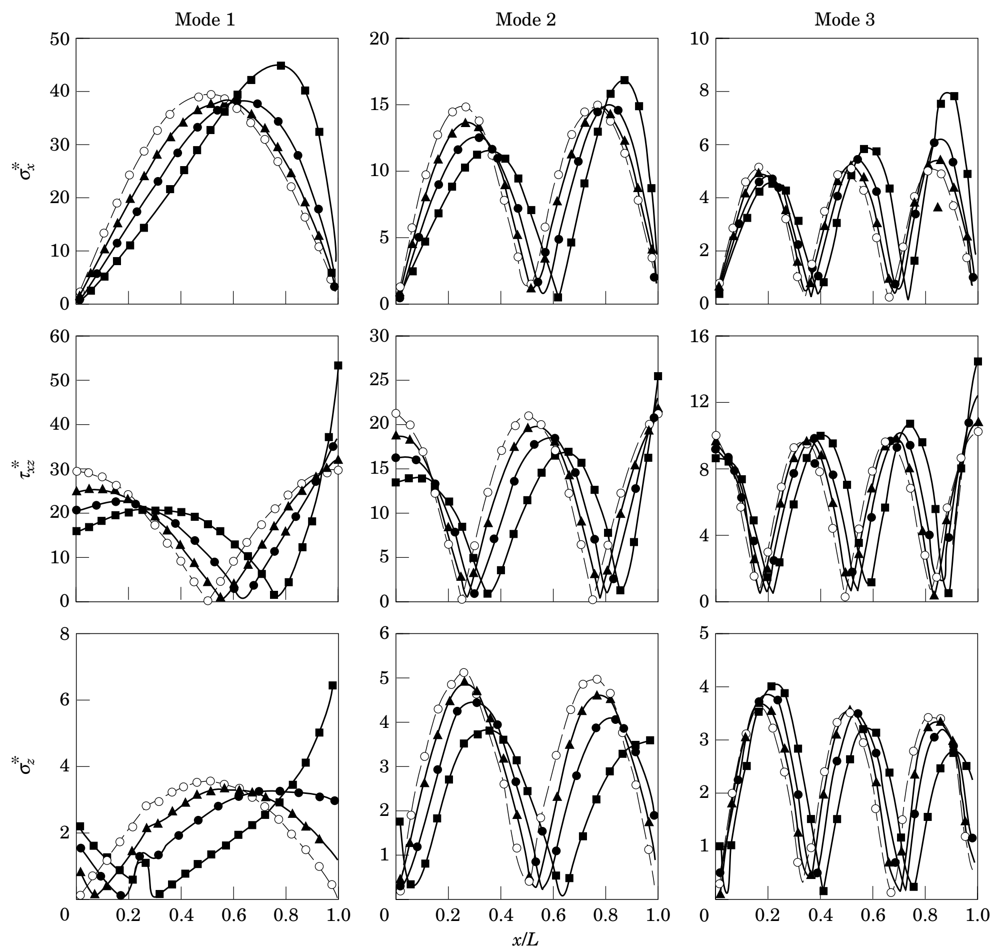

Figure 4. As Figure 3, but decreasing thickness variation.

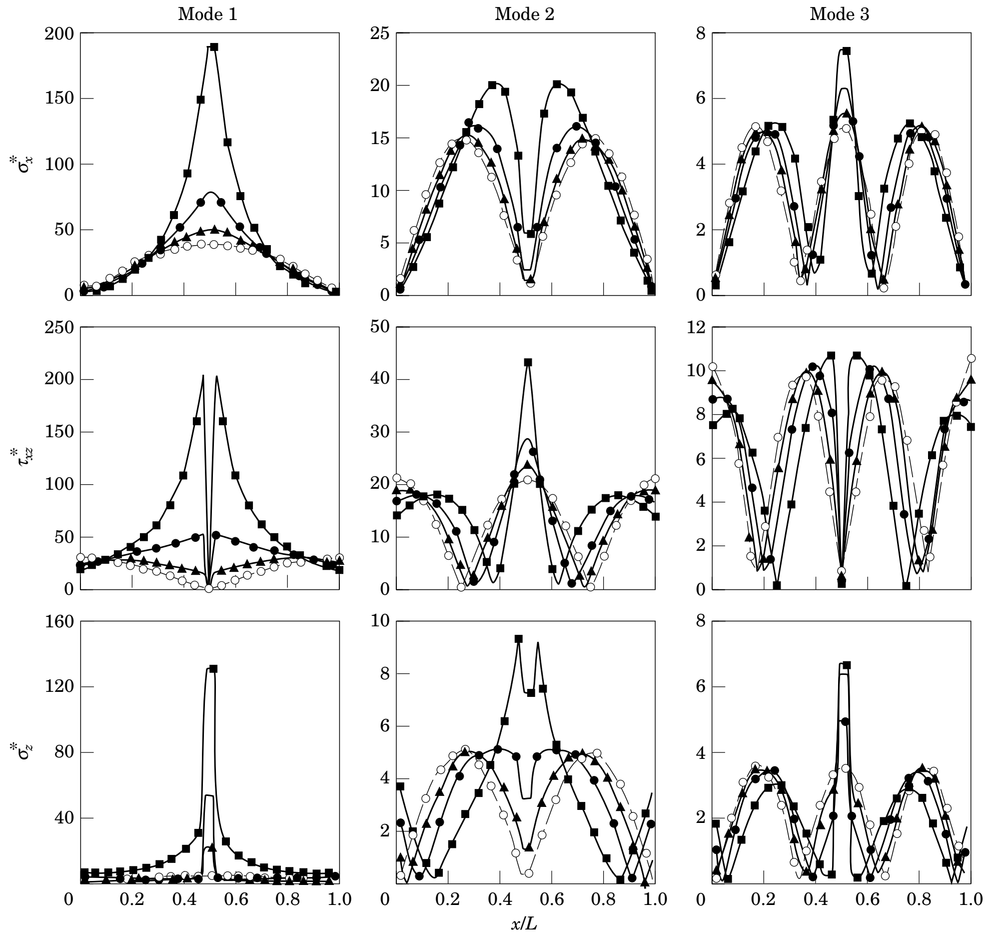

Figure 5. As Figure 3, but decreasing–increasing thickness variation.

in a uniform beam. However, there is little change in the interlaminar stresses developed. But for taper parameters greater than 0·5 the deflection and stresses developed in a decreasing thickness beam are higher than those developed in a uniform beam.

For any particular taper parameter, with the exception of very low taper parameters, τ_{xz} developed in a decreasing thickness variation beam is lower than that developed for the other thickness variations considered. At lower taper parameters the shear stress developed in a decreasing–increasing thickness variation beam is slightly lower than that developed for decreasing thickness variation. At higher taper parameters the shear stress developed in beams with decreasing–increasing as well as increasing–decreasing thickness variations is very high due to the sudden change of cross-section.

The maximum interlaminar normal stresses σ_z developed for both increasing and decreasing thickness variations are more or less the same. The maximum σ_z developed for decreasing–increasing and increasing–decreasing thickness variations, especially at higher taper parameters, is very high, due to the sudden change of cross-section. There is little variation in the maximum value of σ_z at higher modes for all thickness variations.

3.1.2. *Effect of taper parameter*

The frequency decreases with the increase in taper parameter in cases of increasing decreasing and decreasing–increasing thickness variations. In the case of increasing–decreasing thickness variation, the frequency slightly increases as the taper parameter increases for $0 < \beta < 0{\cdot}5$ and then decreases for $\beta > 0{\cdot}5$. As far as free vibration is concerned, the behaviours for increasing and decreasing thickness variations are the same and hence the frequencies obtained for increasing and decreasing thickness variations are the same.

The maximum transverse displacement w_{max} increases with the increase in taper parameter in the case of decreasing, increasing and decreasing–increasing thickness variations. However, in the case of increasing–decreasing thickness variation w_{max} decreases with an increase in the taper parameter for $0 < \beta < 0{\cdot}5$ and for a taper parameter greater than 0·5 there is a slight increase in w_{max} as the taper parameter increases.

A similar trend as that observed in the w_{max} variation with taper parameter is also observed in the variation of the maximum value of σ_x. The maximum values of the

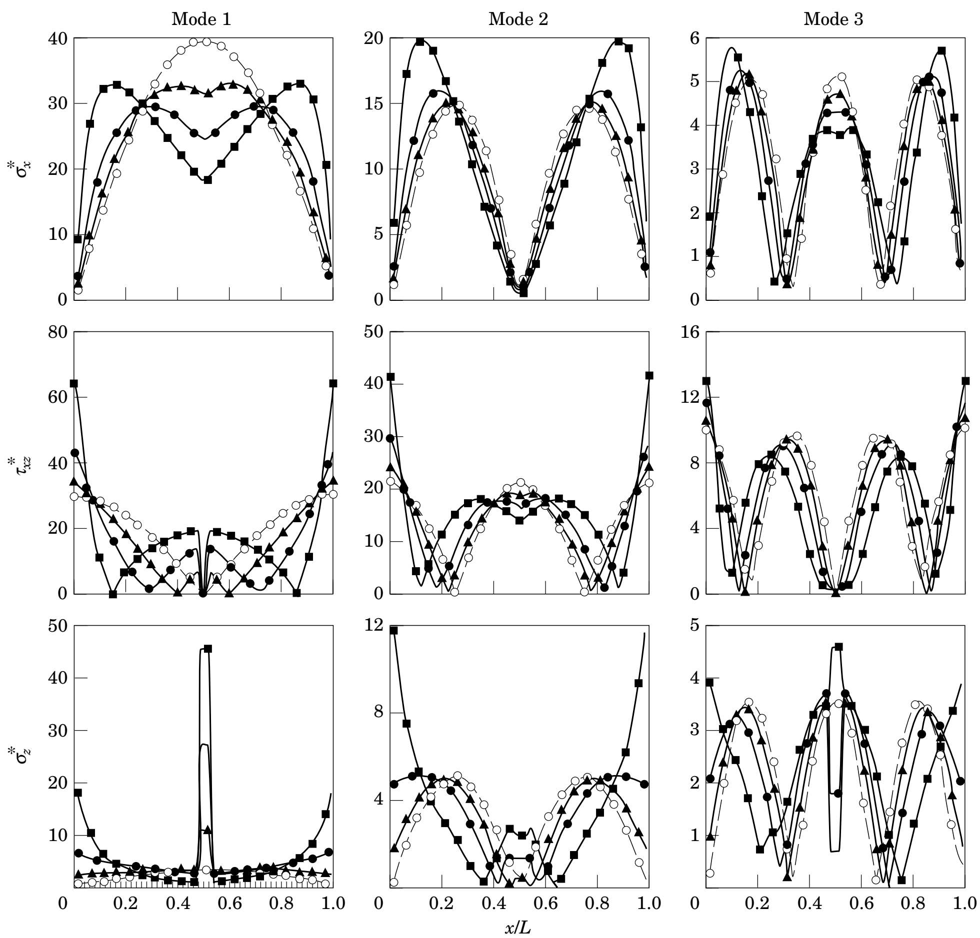

Figure 6. As Figure 3, but increasing–decreasing thickness variation.

interlaminar stresses developed increase with the increase in taper parameter. The deflections and stresses induced are very high for taper parameters well above 0·5. The introduction of taper results in the development of an interlaminar normal stress σ_z at the free edges.

4. CONCLUSIONS

A number of results have been presented to show the effect of the taper profile and the taper parameter on the harmonic response of laminted composite beams. The validity of the present results has been established by comparisons with existing results. Comparison of results shows that there is little deviation in the results predicted by HSDT and FSDT. The introduction of taper results in the development of interlaminar normal stress at the free edges. Despite some minor advantages gained in the cases of decreasing and increasing–decreasing variations, there is little advantage to be gained for tapered beams with simply supported boundary conditions.

REFERENCES

1. R. K. Kapania and S. Raciti 1989 *American Institute of Aeronautics and Astronautics Journal* **27**, 935–946. Recent advances in analysis of laminated beams and plates, part-II: vibrations and wave propagation.
2. F. Yuan and R. E. Miller 1989 *Computers and Structures* **31**, 731–745. A new finite element for laminated composite beams.
3. F. Yuan and R. E. Miller 1990 *Composite Strucutres* **14**, 125–150. A higher-order finite element for laminated beams.
4. B. S. Manjunatha and T. Kant 1993 *Composite Structures* **23**, 61–73. New theories for symmetric/unsymmetric composite and sandwich beams with C^0 finite element.
5. C. Lee and D. Liu 1992 *Computers and Structures* **42**, 69–78. An interlaminar stress continuity theory for laminated composite analysis.
6. D. L. Karabalis and D. E. Beskos 1983 *Computers and Structures* **16**, 731–748. Static, dynamic and stability analysis of structures composed of tapered beams.
7. S. Oral 1991 *Computers and Stuctures* **38**, 353–360. A shear flexible finite element for non-uniform laminated composite beams.
8. A. K. Miller and D. F. Adams 1975 *Journal of Sound and Vibration* **41**, 433–449. An analytic means of determining the flexural and torsional resonant frequencies of generally orthotropic beams.
9. J. R. Vinson and R. L. Sierakowski 1986 *Behaviour of Structures Composed of Composite Materials*. Martinus Nijhoff. See pp. 139–144.
10. A. T. Chen and T. Y. Yang 1985 *Journal of Composite Materials* **19**, 459–475. Static and dynamic formulation of symmetrically laminated beam finite element for microcomputer.
11. K. Chandrashekhara, K. Krishnamurthy and S. Roy 1990 *Composite Structures* **14**, 269–279. Free vibration of composite beams including rotary inertia and shear deformation.
12. K. Chandrashekhara and K. M. Bangera 1992 *Computers and Structures* **43**, 719–727. Free vibration of composite beams using a refined shear flexible beam element.
13. A. Bhimaraddi and K. Chandrashekhara 1991 *Composite Structures* **19**, 371–380. Some observations on the modeling of laminated composite beams with general lay-ups.
14. J. N. Reddy 1984 *Journal of Applied Mechanics* **51**, 745–752. A simple higher order theory for laminated composite plates.
15. T. Kant and B. S. Manjunatha 1994 *Computers and Structures* **50**, 351–365. On accurate estimation of transverse stresses in multilayer laminates.
16. G. B. Warburton 1976 *The Dynamical Behaviour of Structures*. Oxford: Pergamon Press. See pp. 131–133.

APPENDIX: FUNCTIONS FOR THE VARIOUS THICKNESS VARIATIONS CONSIDERED

Linear, increasing,

$$f(x) = 1 - x/L;$$

linear, decreasing,

$$f(x) = x/L;$$

linear, increasing–decreasing,

$$f(x) = 2x/L, \qquad \text{for } 0 \leqslant x \leqslant L/2,$$

$$f(x) = 2(1 - x/L), \qquad \text{for } L/2 \leqslant x \leqslant L;$$

linear, decreasing-increasing

$$f(x) = 1 - 2x/L, \qquad \text{for } 0 \leqslant x \leqslant L/2,$$

$$f(x) = -(1 - 2x/L), \qquad \text{for } L/2 \leqslant x \leqslant L;$$

parabolic, increasing,

$$f(x) = 1 - (x/L)^2;$$

parabolic, decreasing,

$$f(x) = 1 - (1 - x/L)^2;$$

parabolic, decreasing–increasing,

$$f(x) = 1 - (2x/L - 1)^2;$$

parabolic, increasing–decreasing,

$$f(x) = (1 - 2x/L)^2.$$